REPRINTED FROM:

Experimental Heat Transfer, Fluid Mechanics and Thermodynamics 1993

Volume 1

Proceedings of the Third World Conference on
Experimental Heat Transfer, Fluid Mechanics and Thermodynamics
Honolulu, Hawaii, USA, 31 October-5 November, 1993

Experimental Heat Transfer, Fluid Mechanics and Thermodynamics 1993
M.D. Kelleher et al. (Editors)
© 1993 Elsevier Science Publishers B.V. All rights reserved.

THERMAL CHARACTERISTICS OF NATURAL CONVECTION COOLED FIN-TUBE HEAT EXCHANGER

N. Kayansayan
Department of Mechanical Engineering
Dokuz Eylul University, Bornova 35100, Izmir, Turkey

1993
ELSEVIER
AMSTERDAM • LONDON • NEW YORK • TOKYO

Experimental Heat Transfer, Fluid Mechanics and Thermodynamics 1993
M.D. Kelleher et al. (Editors)

© 1993 Elsevier Science Publishers B.V. All rights reserved.

THERMAL CHARACTERISTICS OF NATURAL CONVECTION COOLED FIN-TUBE HEAT EXCHANGER

N. Kayansayan
Department of Mechanical Engineering
Dokuz Eylul University, Bornova 35100, Izmir, Turkey

ABSTRACT

There are numerous instances where the heat transfer from a fin-and-tube heat exchanger to air takes place primarily via natural convection. The lack of data showing the effect of the fin spacing, the fin length and the Rayleigh number on the thermal performance of the exchanger prompted this experimentation. It was found that the interaction of the fin boundary layer with the tube-base brought about a reduction in the Nusselt number and in the convection-conductance value of the finned surface relative to that for the classical case of the long isolated cylinder. At Rayleigh numbers beyond the critical, the Nusselt number was quite insensitive to the fin spacing and length with the typical data spread being in the 5-10 percent range. For a given temperature difference, the occurrence of an optimum fin spacing ratio is indicated.

INTRODUCTION

Natural convection heat exchange devices, such as those employed in dissipating heat from refrigeration units to the surrounding still air or in cooling of cylinder-like electronic components, may involve the interaction of buoyant streams individually induced by various surfaces which comprise the device. A proper formulation of natural convective heat transfer coefficients presents difficulties for a unit consisting of a bank of finned tubes as shown in Fig.1. In addition to radiative heat interactions between the finned tubes and the casing wall, as the buoyancy-induced flow proceeds through the exchanger, successive merging and disruption of air plumes generated by the heated tubes will take place. This complex physical situation is the subject of the present work in which the thermal performance of a single horizontal finned tube in still air was investigated experimentally.

The experiments were performed with a highly polished, isothermal horizontal cylinder serving as the host surface for the vertical circular fins which were also polished to a mirror-like finish. Three parameters were varied during the course of the experiments. One of these is fin spacing, s. At each fixed spacing, the temperature difference between the cylindrical surface and the ambient was varied systematically, so that the cylinder Rayleigh number, Ra, ranged from about 10^5 to 10^8. Four values of D/d, the ratio of the fin diameter to the tube diameter, 1.5, 2.0, 3.0 and 6.0 were used.

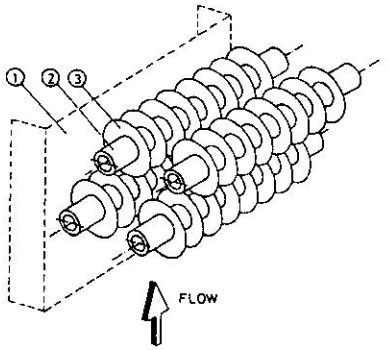

Fig.1 Sketch of a heat exchanger operated in natural convection mode.

A search of the literature failed to reveal any published work related to the subject of the present research. Studies related to systems of parallel or staggered fins attached to a vertical plate are well documented [1,2]. In a review by Incropera [3], studies which dealt with interactions between pin-fin arrays in air with and without shrouds are summarized.

EXPERIMENTAL SETUP AND PROCEDURE

A schematic of the experimental apparatus is presented in Fig.2. The stainless steel heating element located at the center of the system is 24 mm diameter, 600 ∓ 3 mm long, with a wall thickness of 4 mm. The tube accommodates a 15 mm diameter ceramic core with a spiral 4 grooves per cm, machined to 1.5 mm in depth on its periphery. In the design of the heater, the choice of the heating wire was made to attain the highest possible resistance, and thereby to keep the electric current flow as small as possible. A nichrome wire, 10 m in length and 0.5 mm in diameter with resistivity of 10^{-4} ohm.cm, was installed in the ceramic grooves to provide the uniform heating along the tube axis. To reduce the possible extraneous heat losses by conduction, 0.5 mm diameter copper lead wires were used to deliver the power to the heater. For the same

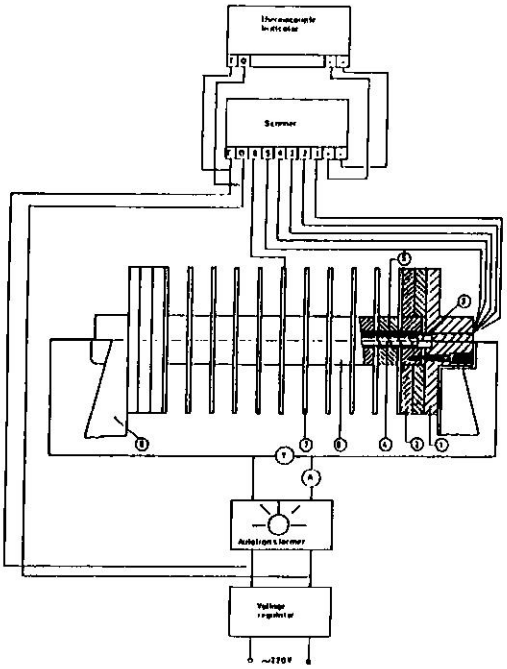

Fig.2 Schematic diagram of the experimental apparatus.

reason, the voltage tap wires used for measuring the voltage drop across the heating element were of 0.1 mm diameter constantan.

To facilitate the variation of fin spacing, pure aluminum collars with two different widths of 12.5 mm and 25 mm were machined and polished on a lathe. Thus, the outside diameters being 200 mm, 150 mm, 100 mm, and 50 mm, a total of eight different types of cylindrical collars have been constructed. Each collar has a central hole of 24 mm in diameter bored with 0.1 mm tolerance which ensures a snug fit around the heating tube, and a 2 mm hole drilled along the radial direction provides an accommodation for a thermocouple wire measuring the surface temperature. Slots, 5 mm deep by 10 mm wide, machined on the central bore hole of the collars yield an internal housing channel for the thermocouple wires.

As shown in Fig.2, the exchanger assembly was compressed by bakelite nuts fitted on the ends of the stainless steel tubing, thus good thermal contact between the collars and the fins was obtained. The ends of the assembly were completely insulated with a layer of styrofoam backed by wooden shrouds.

Figure 3 shows the fin layout and the thermocouple arrangement. The characteristics of the thermocouple wire, i.e. small diameter, high sensitivity, were selected with a view toward minimizing resolution of small temperature differences. This objective was fulfilled by 0.3 mm diameter fiberglass coated copper constantan

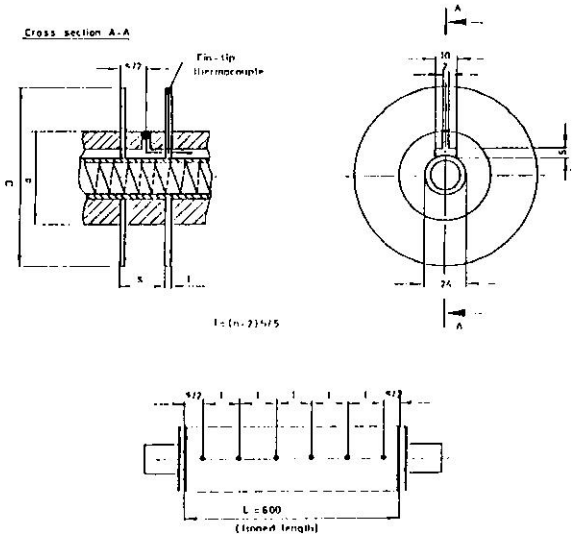

Fig. 3 Exchanger characteristic geometry and the thermocouple arrangement.

wire that was specially calibrated for these experiments. Each of the test configurations was equipped with seven thermocouples. Six of these thermocouples were positioned along the cylindrical surface such that the two were at a distance of s/2 from the ends of the exchanger and the others with approximate intervals of (n-2)s/5 were at mid-sections of the collars. These thermocouples were so installed through the 2 mm openings of the aluminum collars and fixed to the surface with copper-oxide cement that there was precise axial alignment along the fin-tube assembly. The seventh thermocouple measured the tip temperature of a fin at the mid-section of the assembly. The temperature of the ambient air was sensed (and possible stratificaiton detected) by a vertical array of three thermocouples. Being 50 cm apart from each other in the vertical direction, these thermocouples were completely shielded with regard to the radiation from the apparatus. After passing through a scanner system, the thermocouple emf outputs were read by a 4 1/2 digit digital voltmeter which had been used in the thermocouple calibration. All thermocouple interfaces, i.e. connectors and terminals, were maintained spatially isothermal by means of an enveloping aluminum block.

Power for the heater was provided by a regulated a-c supply having a capacity of 2 kW and a stability of 0.5 percent over a three day period. The power circuitry involved an autotransformer for voltage control. All heater related voltages, and current were measured with a digital voltmeter and an ampermeter which had been calibrated with AC/DC calibration standard and both instruments had a rated accuracy of $\mp$ 0.2 percent of the reading.

Table 1 Finned tube test dimensions

Configuration number (-)	Fin diameter D (mm)	Fin thickness t (mm)	Tube diameter d (mm)	Fin spacing s(mm)	Number of fins n (-)	Exchanger finning factor α (-)
1	300	2	200	12.5	49	11.090
2	300	2	200	25	25	5.925
3	300	2	200	50	13	3.531
4	300	2	200	100	7	2.268
5	300	2	200	200	4	1.638
6	300	2	150	37.5	17	5.305
7	300	2	150	75	9	3.031
8	300	2	150	150	5	1.893
9	300	2	100	12.5	49	16.707
10	300	2	100	25	25	8.606
11	300	2	100	50	13	4.555
12	300	2	100	100	7	2.529
13	300	2	50	12.5	49	71.855
14	300	2	50	25	25	36.438
15	300	2	50	50	13	24.011

The experimental apparatus was situated in a laboratory of dimensions, 4.3 m x 7.6 m x 3 m, which possessed remarkable thermal isolation and stability characteristics. The laboratory is, in fact, a room within a room. Its walls, ceiling and floor are each backed by a 20 cm thickness of cork which provides excellent thermal isolation. There are no ducts, grilles, vents, or heating pipes in the laboratory. Thermal stratification, even after long data runs, was negligible. To ensure the absence of disturbances in the laboratory, all instrumentation and power supplies were situated in a room adjacent to the laboratory.

In determining the effect of geometrical parameters on heat transfer characteristics of the exchanger, many experiments have been carried out on different dimensions (Table 1). Each data run was initiated by setting the heater power inputs at levels which would yield the desired surface-to-ambient temperature difference. Then, an equilibration period of at least eight hours was allowed before any readings were made. In addition to the power consumption, the laboratory air, cylinder surface and fin-tip temperatures were recorded. After rotating the fin-tube assembly 60 degrees about its axis, and allowing sufficient time for the reinstatement of steady state flow conditions, cylinder wall temperatures were recorded.

A note was taken of the degree of temperature deviations along the cylindrical surface. In principle, to establish identical flow conditions on the axial direction of the test exchanger, the measured longitudinal temperatures at a particular run should be equal. In experiments, specifically at high power inputs, the maximum temperature deviation was calculated to be 2.7 percent of the wall-to-ambient temperature difference ΔT.

DATA REDUCTION

The procedures used to determine the finned-tube heat transfer coefficients, Nusselt numbers, and Rayleigh numbers from the thermocouple outputs, power input and barometric pressure will now be described. The starting point of the data reduction procedure is the definition of the average heat transfer coefficient for the finned surface,

$$h = \frac{Q}{\eta A (T_w - T_\infty)} \qquad (1)$$

where Q is the rate of heat transfer by natural convection from the surface to the air, and A is the total exposed surface area, including the fin tip face, expressed as follows,

$$A = \left(\frac{\pi}{2}\right)(n-1)d^2\left[\left(\frac{D}{d}\right)^2 + 2\left(\frac{s}{d}\right) + 2\left(\frac{n}{n-1}\cdot\frac{D}{d} - 1\right)\left(\frac{t}{d}\right) - 1\right] \qquad (2)$$

In equation (1), η represents the total surface temperature effectiveness [4] and is defined as,

$$\eta = 1 - \frac{A_f}{A}(1 - \eta_f) \qquad (3)$$

The average of six thermocouple readings on both longitudinal and circumferential directions was used to evaluate T_w in eq. (1).

The electric power input to the heater is equal to the sum of the rates of heat transfer from the exchanger assembly by natural convection and by radiation. If E and I recpectively denote the measured voltage and current for the heater and Q_r is the radiation heat transfer from the cylindrical finned surface, then,

$$Q = EI - Q_r \tag{4}$$

The fin-tip to ambient temperature difference, ΔT_{ft}, is expressed as a percentage of ΔT, for most experiments then deviations on the tip temperature difference were in the range from 6 to 14 percent of the base temperature difference ΔT. At the geometrical configuration for which D/d was 6.0, and only high power inputs, a maximum of 16 percent deviation was detected. Consequently, in radiative heat loss analysis, the fins, within acceptable engineering accuracy, can be assumed to be at a uniform temperature which is evaluated as the average of the base and the tip values.

As shown in Fig.4, an enclosure confined by two adjacent fins, the collar in between, and the imaginary black surface, S4, complete the unit cell for radiation analysis. The radiant energy flux streaming through the cell can be regarded as having two components. One of these stems from the black surface S4. The other stems from the fin-tip surface owing to a temperature different from the temperature of the room. These two constributions to Q_r are respectively designated as Q_{r1}, and Q_{r2}. The heat loss through the fictive surface S4 is,

$$Q_{r1} = \pi D\,(s - t)\,(n - 1)\,q_4 \tag{5}$$

where, q_4 represents the net radiant flux through the surface S4, and the details in relating this flux to the measured properties are studied. Furthermore, the radiation exchange between the fin-tip surface; the surface S3 in Fig.4, and the room is,

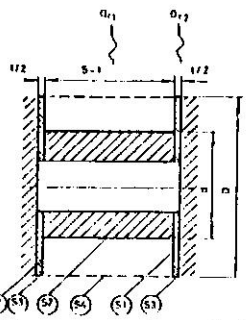

Fig.4 Unit enclosure for radiation analysis.

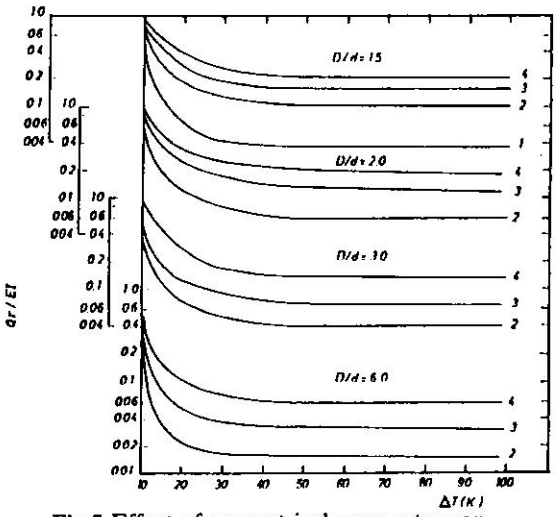

Fig.5 Effect of geometrical parameters on radiative heat loss fraction. ϒ: 1, 0.0625; 2, 0.25; 3, 0.50; 4, 1.00.

$$Q_{r2} = \pi D t n \sigma \varepsilon_{ft} (T_{ft}^4 - T_\infty^4) \tag{6}$$

Equations (5) and (6) may now be added together to yield Q_r. Figure 5 shows the variation of Q_r/EI vs the temperature difference between the wall surface and the ambient for the typical values of fin-to-tube diameter and spacing ratios. The general distribution in this illustration indicates that increase in the temperature difference and/or in the diameter ratio, D/d, drastically decreases the radiation losses and the curve becomes quite flat in the range where ΔT is greater than 25 K.

With the determination of Q_r, the convective heat transfer rate Q follows from eq. (4) and the heat transfer coefficient h is then evaluated from eq. (1). The h values will be reported in dimensionless form via the Nusselt number; hd/k. The results will be parameterized by the Rayleigh number, $g\beta\rho^2 c_p d^3 (T_w - T_\infty)/\mu k$, and by the modified Rayleigh number,

$$Ra^* = Nu.Ra \tag{7}$$

Aside from ß, the thermophysical properties contained in the Nusselt and the Rayleigh number expressions were computed at a reference temperature, T_{re}, suggested in [5],

$$T_{re} = T_w - 0.38\,(T_w - T_\infty) \tag{8}$$

and $\beta = 1/T_\infty$. The measured barometric pressure was used in the determination of the density ρ. The uncertainties in the measured properties were

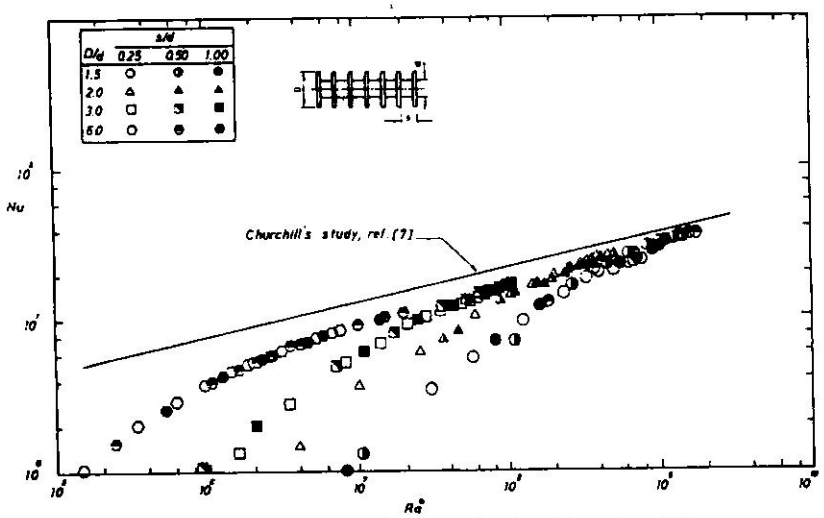

Fig.6 Finned tube natural convection heat transter data and comparison with horizontal cylinder results.

Table 2 Experimental uncertainties

Property	Uncertainty	Range
Surface temperature	± 0.3 K	303 K to 443 K
Ambient temperature	± 0.5 K	293 K to 298 K
Wall temperature difference	± 0.5 K	10 K to 180 K
Power input	± 0.5 W	10 W to 100 W
Power input	± 2.2 W	100 W to 780 W
Total emissivity	± 0.002	0.04 to 0.072

estimated to be as in Table 2. The method of Kline and McClintock [6] was employed in evaluating the uncertainties of the experimental results. For moderate wall-to-ambient temperature difference ($\Delta T \sim 70$ K), the radiation heat losses were found to be within 6 percent, and the heat transfer coefficients within 7 percent of the reported values.

RESULTS AND DISCUSSION

Figure 6 presents the Nusselt number results as a function of the modified Rayleigh number and indicates that as the diameter ratio increases the heat transfer coefficients also increase. This is basically attributed to the up-moving boundary layer flow induced by fins. At large fin diameter ratios, the existence of such an oncoming flow is stronger and reinforces the buoyant flow that is induced by the tube base itself. Thus, the augmented velocity field should give rise to higher heat transfer coefficients.

In direct conflict with the velocity-related enhancement is the preheating effect due to fins. Owing to the heat transfer from the fin to the air that passes along it, the temperature of the fin-induced air flow that arrives at the cylinder surface is heigher than the ambient temperature. Thus, for identical flow conditions, the effective finned tube-to-air temperature difference is less than the temperature difference between the bare tube surface and the ambient. This behavior then tends to degrade the heat transfer coefficients. The extent of the degradation should be greater when the fin diameter ratio is larger, since the preheating effect of the fin increases with its diameter.

Since both the aforementioned opposing effects are especially stronger at high Rayleigh numbers, there should be a limit to increase of heat transfer coefficients. It is evident from Fig.6 that the data points for all diameter ratios approach asymptotically to the horizontal cylinder results. There are a number of competing correlations in the literature for horizontal cylinders. Three of the most accepted correlations have been evaluated for the operating conditions of the present experiments and compared with the present findings. These include: (a) Churchill ([7], eq. (10)), (b) Fand ([8], eq.(17)), (c) Morgan ([9], Table 2). The Churchill correlation, as restated with respect to modified Rayleigh number, is plotted in Fig.6 and displays an upper bound to the present findings.

The general sensitivity of Nu values to D/d is worthy of special note, and Fig.7 may be examined in this regard. Here, Nu x Ra, data for a fin diameter ratio of 3.0 are plotted as a function of Rayleigh number. An interesting feature of this illustration is the existence "discrete transitions". An ad hoc method which has been verified to be succesful in the literature [10, 11] is implemented in locating the transition points. The

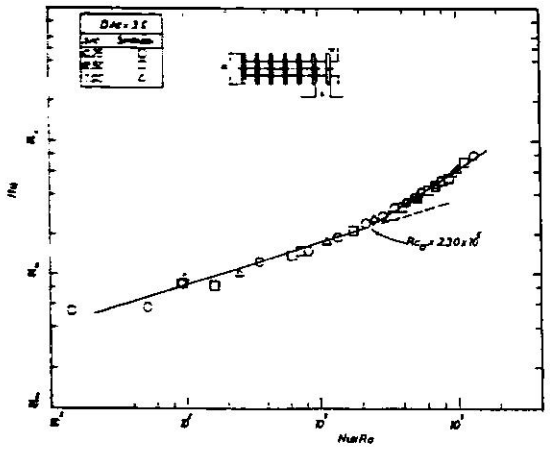

Fig.7 Discrete transition in heat flux for horizontally oriented finned tube.

Table 3 Rayleigh numbers for discrete transitions in heat flux

0.25 ≤ s/d ≤ 1.00		
D/d	Ra_{cr}	$(D/d)^3 \times Ra_{cr}$
1.50	1.78×10^7	6.007×10^7
2.00	0.775×10^7	6.200×10^7
3.00	0.230×10^7	6.210×10^7
6.00	0.028×10^7	6.048×10^7

method considers a change in the slope of a linear curve produced in determining the transition. The critical Rayleigh numbers at transitions are summarized in Table 3. As shown in this table, for spacing ratios in the range from 0.25 to 1.0, the term, $\lambda^3 Ra_{cr}$, with a deviation of ∓ 2 percent, can be stated to be constant for all diameter ratios and approximated to be,

$$\lambda^3 . Ra_{cr} = 6.11 \times 10^7 \qquad (9)$$

The significance of the transition is that no fin boundary layer interference occurs at Rayleigh numbers above critical value, and the data points for all geometric parameters cluster on a single line. As shown in Fig.8, for $Ra > Ra_{cr}$, the effect of the fin diameter and spacing on Nusselt number becomes undetectable in the data presentation. Then, a single equation relating the two principal parameters is determined from a least-squares curve fit and is given by

$$Nu = 0.081\ Ra^{0.336} \qquad (10)$$

This relation is found to be valid for the ranges of parameters indicated by: (i) D/d = 1.5 to 6.0, (ii) s/d = 0.25 to 1.0 and (iii) $Ra > Ra_{cr}$. In equation (10), the exponent is very close to Morgan's result [9] and

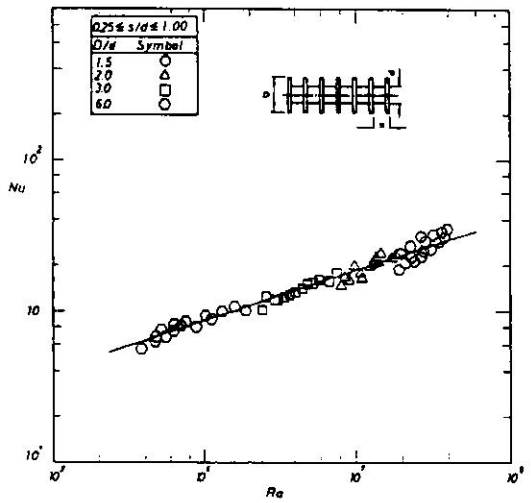

Fig.8 Average Nusselt number results for Rayleigh numbers above the critical

signals, as expected, the lessened influence of fin-tube interaction.

To determine the effect of fin spacing on the performance of the exchanger, the test data were also plotted in the form shown in Fig.9. This figure represents two distinct ordinates plotted against the fin spacing ratio at a temperature difference; ΔT=67 K. One of these ordinates is the finned surface convection conductance value divided by the bare tube convection conductance value and is defined as,

$$\phi = \frac{(\eta hA)}{(hA)_o} \qquad (11)$$

The second ordinate representing the exchanger finning factor α, expresses the ratio of the total finned surface area exposed to air to the plain tube area as follows,

$$\alpha = \frac{A}{A_o} \qquad (12)$$

In Fig.9, as the fin density increases, i.e., s/d << 1 , the convection-conductance ratio does not increase in the same manner as the finning factor does. This result is indicated by the variation of the parameter ϕ / α in the same figure. As the spacing ratio increases, a lesser fraction of the tube base will be affected by the fin boundary layer and a relevant enhancement in ϕ is noted. It may also be seen that for any s/d-value the heat transfer from the finned surface will never be as great as that would be obtained from a plain tube of equal diameter and surface area, i.e., if $\alpha = 1$, then $\phi < 1$ in ϕ / α vs s/d representation. At a particular fin-tube geometry and a temperature difference ΔT, to

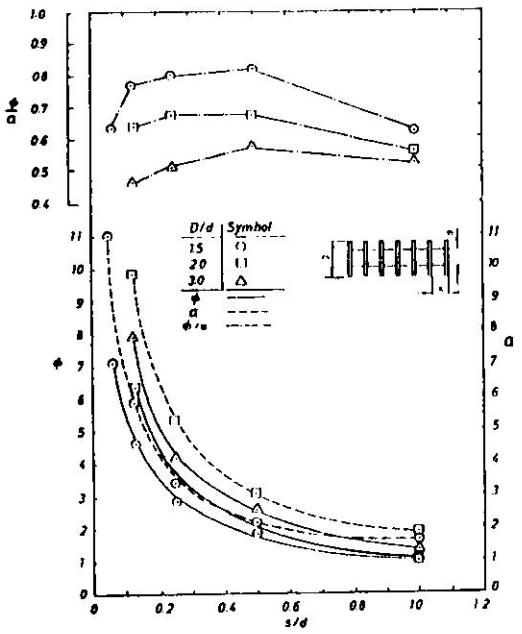

Fig.9 Effect of fin spacing on convection - conductance at ΔT = 67 K.

evaluate the total heat flow rate from the finned surface is practically significant. Figure 10 should be observed in this regard. The "effective" heat transfer coefficient he, which represents the combined convection-radiation heat flux streaming through the finned surface per unit temperature difference, defines the effective Nusselt number, $h_e d/k$, as the ordinate in Fig.10. At a pre-determined Rayleigh number value, the convective Nusselt number can be estimated by using Fig.6 or eq.(10) provided that the surface geometric parameters are in the range as specified in the present study. Then Fig.10 yields the heat transfer coefficient required for calculating the total heat flow rate. In Fig.10, at low Nu-values, scattering in the data is noted. This behavior is attributed to the dominance of the radiative heat transfer in the dissipated heat rate at low temperatures. It may be seen from Fig.5 that in a range for $\Delta T < 25$ K the portion of the total heat input carried away by radiation drops from 70 percent to 10 percent, and strongly depends on the fin-tube configuration. However, due to fairly constant and small contribution of radiation at high ΔT-values; $\Delta T >$ 30 K, the data points in Nu vs Nu_e representation merge to a single line.

CONCLUSION

In the experiments performed here, three physical parameters were varied with a view towards analyzing the natural convection characteristics of the

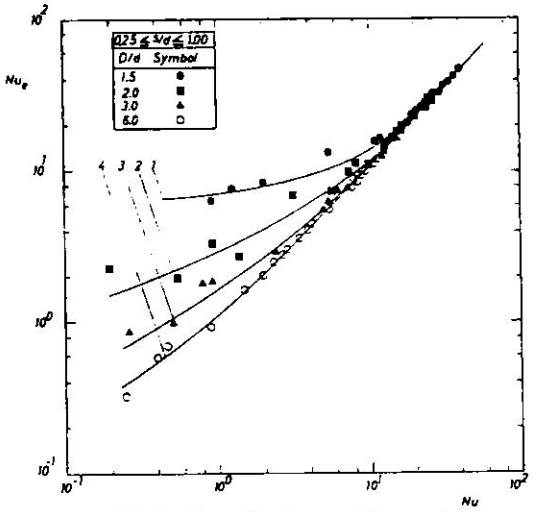

Fig.10 The finned tube total heat rate characteristics. λ: 1, 1.5; 2, 2.0;3, 3.0; 4, 6.0.

horizontally oriented isothermal heat exchanger equipped with constant thickness, circular fins. The varied parameters included the fin spacing ratio ranging from 0.0625 to 1.0, and the fin diameter ratio in the range of 1.5 to 6.0, and the surface-to-fluid temperature difference, i.e. the cylinder Rayleigh number. To provide equi-temperature surfaces, the copper fins and the aluminum collars served as the cylindrical surface and used for the entire experiments. The data which cover the Rayleigh number range from 10^5 to $5x10^7$ are appropriate for most applications of this type of extended surface when transfering heat to air by natural convection.

With regard to the Nusselt number, it tends to be enhanced by the fin-induced approach flow and to be degraded by the fin related preheating of the approach flow. The degrading effect is considerable at low Rayleigh numbers. At high Ra-values, however, the net balance between these two conflicting effects was found to be insensitive to all of the varied geometrical parameters. The critical Rayleigh number marked the transition to this insensitiveness and an abrupt change of slope in Ra^* vs Ra presentation was noticed.

The net effect of the presence of the fins is to degrade the cylinder Nusselt number, as witnessed by the fact that the Nusselt numbers for the finned tube are lower than those for single isolated cylinder. The test data for Rayleigh numbers above the critical value are correlated by eq. (10) which represents the data with a $\mp$ 10 percent deviation.

On the basis of identical surface area and temperature difference, the thermal behavior of the finned tube is compared with a horizontal tube. It is

shown that the convection heat transfer does not increase directly with addition of fin surface area. There is an optimum fin spacing for any fin diameter ratio, above or below which there is a reduction in convection-conductance. Depending upon the temperature difference, the optimum spacing ratio s/d lies in between 0.25 and 0.50.

ACKNOWLEDGMENT

The author wishes to express his appreciation to TEBA, Solar Collectors Manufacturing Inc., Izmir, for their technical support in the development of the experimental set-up.

NOMENCLATURE

A	heat transfer surface area, m^2
c_p	specific heat at constant pressure, kJ/(kg.K)
D	fin diameter, m
d	tube base diameter, m
E	voltage across the heating element, V
F	angle factor, dimensionless
g	gravitational acceleration, m/s^2
h	heat transfer coefficient, $W/(m^2.K)$
I	current through the heating element, A
k	thermal conductivity, dimensionless
Nu	Nusselt number (= hd/k), dimensionless
n	number of fins, dimensionless
Q	natural convection heat transfer rate from the finned tube, W
Q_r	radiation heat transfer rate from the finned tube, W
q	heat flux, W/m^2
$q_{o,i}$	radiosity of i th surface, W/m^2
Ra	Rayleigh number [= $g\beta\rho^2 c_p d^3 (T_w - T_\infty)/(\mu k)$], dimensionless
Ra^*	modified Rayleigh number [Eq.(7)], dimensionless
s	fin spacing, m
T	temperature, K
ΔT	temperature difference, $T_w - T_\infty$, K
t	fin thickness, m

Greek symbols

α	exchanger finning factor [Eq.(12)], dimensionless
β	volumetric coefficient of thermal expansion, 1/K
Δ	difference
ϵ	surface emissivity, dimensionless
γ	fin spacing ratio (= s/d), dimensionless
λ	fin diameter ratio (= D/d), dimensionless
η	efficiency, dimensionless
μ	dynamic viscosity, kg/(m.s)
ρ	density, kg/m^3

Subscripts

cr	critical
e	effective
f	fin
ft	fin-tip
o	bare tube conditions
r	radiation
re	reference
w	wall
∞	ambient conditions

REFERENCES

1. Bar-Cohen, A., and Rohsenow, W. M., "Thermally Optimum Spacing of Vertical, Natural Convection Cooled, Parallel Plates", ASME Journal of Heat Transfer, Vol. 106, pp. 116-123, 1984.
2. Guglielmini, G., Nannei, E., and Tanga, G.,"Natural Convection and Radiation Heat Transfer from Staggered Vertical Fins", Int.J.Heat Mass Transfer, Vol. 30, pp. 1941-1948, 1987.
3. Incropera, F. P., "Convection Heat Transfer in Electronic Equipment Cooling", ASME Journal of Heat Transfer, Vol. 110, pp. 1097-1111, 1988.
4. McQuiston, F. C., and Parker, J. D., Heating, Ventilating, and Air Conditioning-Analysis and Design, 3rd edition, John Wiley, New York, pp. 555-562, 1988.
5. Sparrow. E. M., and Gregg, J. L.,"The Variable Fluid Property Problem In Free Convection",ASME Transactions, Vol. 80, pp. 878-886, 1958.
6. Kline, S. J., and McClintock, F. A., Describing Uncertainties in Single-Sample Experiments", Mech. Eng.,Vol. 75, pp. 3-8, 1953.
7. Churchill, S. W., and Chu, H. H. S.,"Correlating Equations for Laminar and Turbulent Free Convection from a Horizontal Cylinder",Int.J.Heat Mass Transfer, Vol. 18, pp. 1049-1053, 1975.
8. Fand, R. M., Morris, E. W., and Lum, M., "Natural Convection Heat Transfer from Horizontal Cylinders to Air, Water, and Silicone Oils for Rayleigh Numbers between $3x10^2$ and $2x10^7$", Int.J.Heat Mass Transfer, Vol. 20, pp.1173-1184, 1977.
9. Morgan, V. T., "The Overall Convective Heat Transfer from Smooth Circular Cylinders", Advances in Heat Transfer, Vol. 11, Academic Press, New York, pp. 199-264, 1975.
10. Malkus, W. V. R., "Discrete Transitions in Turbulent Convection", Proc. Royal Society, London, Series A, Vol. 225, pp. 185-195, 1975.
11. Kulacki, F. A., and Richards, D. E., "Natural Convection in Plane Layers and Cavities with Volumetric Energy Sources", Natural Convection: Fundamentals and Applications; editors: Kakac, S., Aung, W., and Viskanta, R., Hemisphere, Washington, pp. 179-225, 1985.